Hydrogeochemical Evolution of Groundwater Resource in an Arid Region of Southeast Iran (Ravar plain–Kerman province)

A. Qishlaqi[*1], M. Abdolahi[1], A. Abbasnejad[2]

[1] *Faculty of Earth sciences, Shahrood University of Technology, Shahrood, Islamic Republic of Iran*
[2] *Department of Geology, Faculty of sciences, University of Shahid Bahonar, Kerman, Islamic Republic of Iran*

Abstract

This study was carried out in the Ravar plain, a typical arid zone in southeastern Iran, with the objectives of evaluating hydrochemical quality of the groundwater resources and identifying the processes that modify the groundwater composition. Groundwater samples were collected from representative wells spread over the study area. Major cations and anions along with physico-chemical parameters were measured as per the standard methods. The study approach includes conventional graphical plots and multivariate analysis of the hydrochemical data to define the hydrogeochemical evaluation of groundwater system based on the ionic constituents, water types and hydrochemical facies. The results indicated that the groundwater in the study area is alkaline (pH 7.1–7.8), hard (TH 350-4000 mg/l) and brackish (TDS 868–13000 mg/l). The Chadha's diagram shows that the prevalent water type is Na–Cl–SO$_4$, with alkali metals exceeding the alkaline earth metals. Gibbs and Durov diagrams as well as ionic ratio plots indicated that evaporation, water–rock interaction and ion exchange are the main processes that regulate the groundwater quality. It was also found that the majority of groundwater samples are undersaturated with respect to evaporitic minerals and oversaturated with respect to carbonate minerals. The application of principal component analysis resulted in two PCs. PC I with loading on Cl-, Na+, SO$_4^{-2}$, EC, and Ca^{+2} which is related to degree of groundwater mineralization while PC II with opposite loadings of HCO$_3^-$ and pH. The findings of the study may be applicable to areas with similar characteristics elsewhere in arid regions.

Keywords: Hydrogeochemical processes; Groundwater resource; Ravar plain; Kerman; Iran.

Introduction

By definition, arid regions are areas with an aridity index of less than 0.2 which is characterized by limited rainfall and high rates of evaporation [1]. These conditions prevail over most parts of the Middle East and Asia. In such areas, surface water resources are extremely scarce and groundwater is often the only

---

source of water for drinking and irrigation purposes. Groundwater resources in arid zones universally suffer from problems of over-abstraction and declining water tables. In addition to the issues related to quantity, degradation of groundwater quality now assumes major importance in arid and semiarid regions.

Generally, quality of groundwater in a region depends on the chemical composition of recharge water, the interaction between water and soil, the types of rock with which it comes into contact in the unsaturated zone, the residence time of groundwater in the subsurface environment and anthropogenic activities (such as agriculture, industry, urban development) [2,3]. Many arid lands, however, have different topographic, climatic, and geologic settings, and other processes may control groundwater compositions. In these areas, low precipitation combined with high rates of evapotranspiration, dissolution of evaporites and intrusion of saline waters can significantly change the groundwater quality. Over the time, these factors in concert with human-related activities (particularly over exploitation) can lead to groundwater salinization which is one of the most conspicuous phenomena of water-quality degradation in many arid and semi-arid zones in the world. The poor quality of groundwater in such environments results in restrictions and limitations on its use and management, and is an impediment to regional economic development.

Given the importance of groundwater quality and to utilize and protect these valuable water resources in arid-semiarid regions, it is necessary to have a comprehensive insight into mechanisms which control groundwater composition under natural water circulation processes. The hydrogeochemical approaches help to get such an insight. Hydrogeochemistry (chemical hydrogeology, geo-chemical hydrology) is an interdisciplinary science that relates the quality of groundwater to various processes and reactions in aquifers. In these methods, water chemistry and (or its isotopic composition) are used as a forensic tool to determine the source of groundwater, to estimate the residence time of water in an aquifer, to identify minerals make-up of aquifer materials and to evaluate the geochemical processes that control the water chemistry along its flow path. These techniques can be applied for defining and mitigating several key water issues including salinization in the arid zones. Knowledge on hydrogeochemistry is also more important to assess the quality of groundwater for understanding its suitability for various needs.

Iran as a dry country is located in the mid-latitude belt of arid and semi-arid regions of the Earth and almost over 60% of its land area is covered by arid and semi-arid regions [4]. Groundwater provides more than half of the total annual water demand in Iran. In recent years, intense agricultural and urban developments together with natural factors have adversely affected the quality and quantity of Iran's subsurface water resources. This is particularly true in Kerman province (southeast of Iran) which is situated on the verge of two main deserts (the Central Desert on the north and Lut Desert on the East) and is facing the problem of groundwater depletion and quality deterioration. Despite the critical importance of groundwater resources in these areas, hydrogeochemical data on these resources is severely limited. This study was carried out in the Raver plain, a typical arid zone in northern Kerman, with the objectives of determining the hydrogeochemical nature of the groundwater in this region and identifying the geochemical processes responsible for the present status of groundwater quality in this area. The findings of the study may be applicable to areas with similar characteristics elsewhere in arid regions.

Materials and Methods

Study area

The study area lies between longitudes 57°,00'–56°,30', 00" E and latitudes 31°,00'–31°,30',00''N (Figure 1) and is located at 140 km north of Kerman city (Kerman province, southeast of Iran). The Ravar plain with an average altitude of about 1170 m above sea level (a.s.l) covers a total area of approximately 4080 km^2 and forms a roughly rectangular depression in the north of Ravar town. The plain is bounded to south and east by a NW-SE trending mountainous belt separating the plain from the Lut Desert. Owing to proximity to this desert, the climate of the study area is arid with hot dry summers and cold dry winters. According to Köppen's climate classification, eastern and central part of the study area have BWSAH (hot desert) climate whereas the southern and western mountainous portions possess BWSAK (cold desert) climate type. Based on the data of the Ravar meteorological station, the average annual temperature ranges from 42 C° in summer to -10 C° in winter. Precipitation, which is the main source of groundwater recharge in the plain, averages 70 mm/yr. More than 70% of the total annual precipitation falls between January and March. The rainfall progressively decreases towards the east as moving to the Lut Desert. The annual potential evaporation is also estimated to be about 3766 mm/year which far exceeds rainfall for this area.
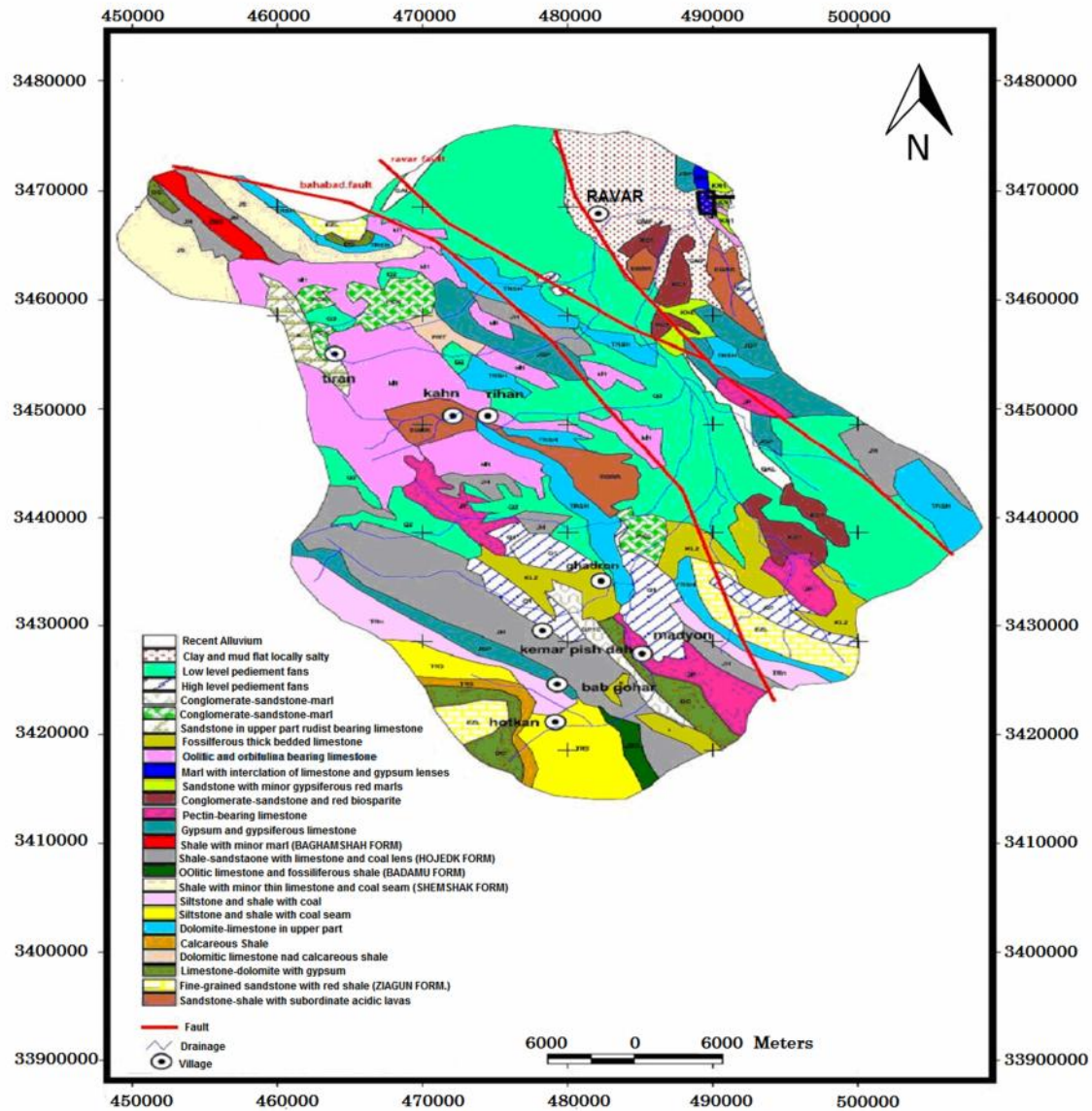
Figure 1. Geological map of watershed (catchment) of the Ravar plain (adapted from [23] with minor modification)

Geology of the study area

Geologically, the study area falls in the central zone of Iran. The geologic formations in the study area range in age from Precambrian to Quaternary and include mostly sedimentary rocks as well as unconsolidated sediments (Figure 1). The main feature is the presence and abundance of evaporitic rock units that are important in terms of groundwater quality. According to Mahdavi et al. (1996) [5] and Stocklin (1961) [6], the evaporite-bearing rock units of this region in descending order by age are as follows (Figure 2):

Dezu series (Middle Cambrian): gypsum and gypsiferous marl with subordinate dolomite intercalations

Shemshak formation (Upper Triassic-Lower Jurassic): an association of sandstone, siltstone, black shale and claystone, variously alternating with thin coal seams, and evaporite-bearing red beds.

Bidu group (Late Jurassic to Early Cretaceous): succession of shale, calcareous sandstone, gypsiferous marl, limestone, and varicolored conglomerate.

Ravar series (Late Jurassic-Early Cretaceous): varicolored intercalation of evaporites (gypsum, and some rock salt), gypsiferous marls, and violet sandstones.

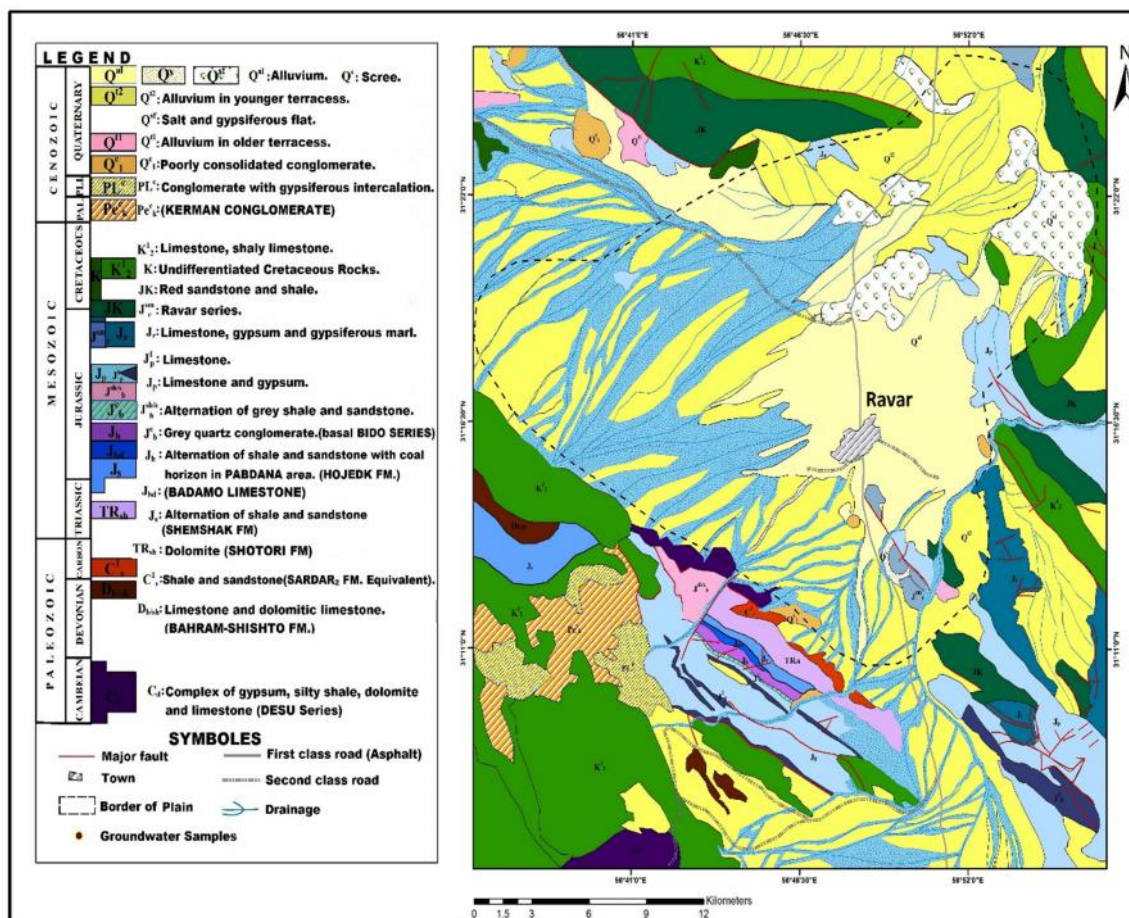*Undifferentiated rock units of Cretaceous age*:

Figure 2. A detailed geological map showing the main lithological units in the study area

limestone, shale, argillaceous limestone with intercalated layers of gypsum.

Kerman conglomerate (Paleocene): Conglomerate, micro-conglomerate, sandstone interlayered with gypsiferous marls.

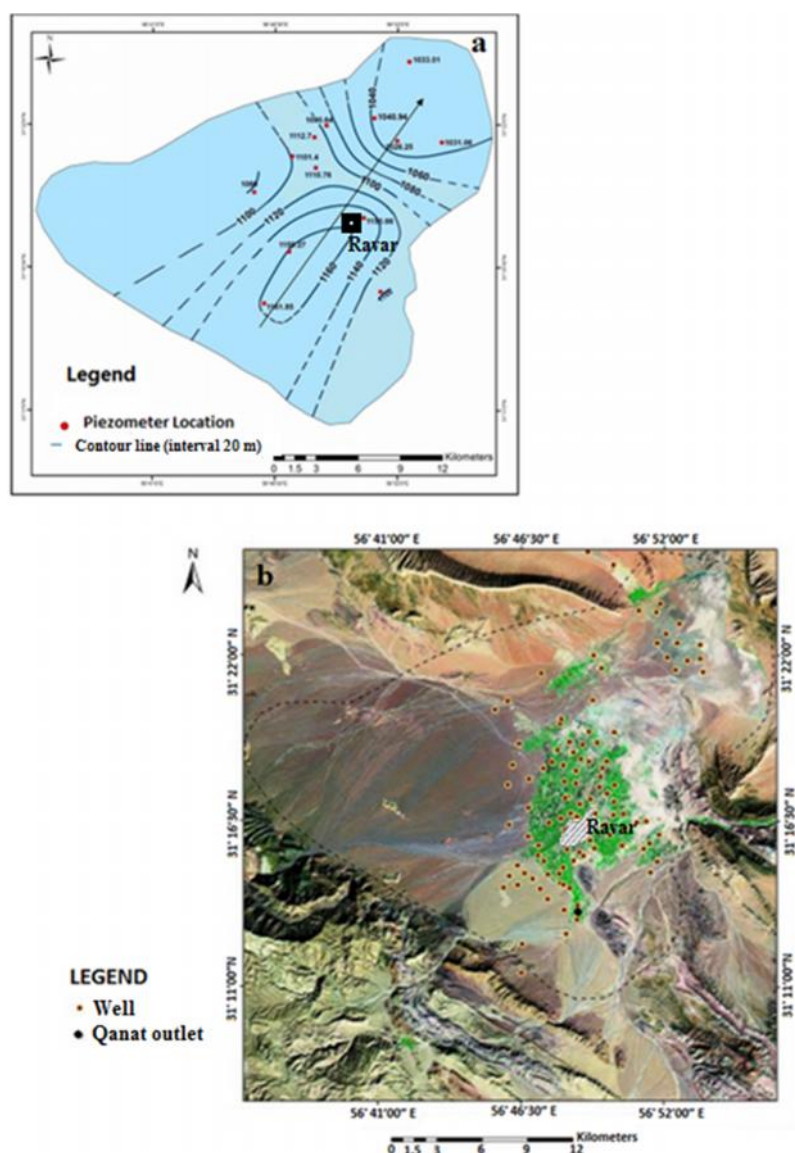*Pliocene conglomerate*: conglomerate intercalated layers of gypsum.

Quaternary deposits: recent alluvium: ancient alluvium fans, sand dunes, and salt-gypsiferous mudflat sediments. The western half of the Ravar plain is mainly covered by a series of coalescing alluvial fans, which forms a broad *Bajada* along the mountains front. The eastern side of the plain is occupied by Playa sediments, which are composed of clay, silt, and abundant evaporitic minerals (e.g. halite and gypsum) formed via co-occurrence of capillary rise and evaporation in the desert environment. So, there are many evaporite-bearing rock units in the stratigraphic record of this region which may be attributed to the geographical location and aridity of this region. Generally, in these evaporites, gypsum is much more widespread than

halite.

Hydrogeology of the study area

From a hydrogeological point of view, the groundwater occurs under unconfined condition in the Quaternary alluviums. To the west and the middle of the plain, the alluvium thickness gradually increases. It is thought that bedrock of the plain is of Jurassic rock units composed mainly of coal-bearing shales and evaporites. The recharge to this aquifer takes place from elevated areas in the south and west. The net annual recharge during 2009-2010 is estimated to be 3×10^3 m^3. Near the playa center; evapotranspiration constitutes the major flux of water out of the system.

The piezometric map of the Quaternary aquifer, based on September 2009 data shows that the groundwater flows from the southwestern highlands towards the northeast (Figure 3a). The groundwater level is typically more than 60 m below ground surface in the west and 4 m in the east, with an overall hydraulic gradient of ca 0.002. Due to climatic aridity, surface

Figure 3. (a) Iso-potential map of the groundwater system in the Ravar plain (the arrow indicates groundwater flow direction). (b) Distribution of abstraction wells and Qantas (outlet) in the study area

water is scarce in the study area. Within the Ravar plain, there are 74 wells and 1 Qantas with total discharge of 72.45×10^3 m^3 (Figure 3b). The majority of existing wells were died up over the past years due to over-abstraction of groundwater.

Sampling and chemical analysis

Out of 74 groundwater wells in the specified area, only 25 wells are working which are used for domestic and/or irrigation purposes. Samples were collected from these abstraction wells in such a way that they represent the entire Ravar plain. Sampling and field measurements were undertaken after purging several well volumes. Groundwater samples were collected in clean polyethylene (HDPE) bottles and were filtered using 0.45-lm pore-size membrane filters (Millipore) to remove suspended particles. The parameters pH, EC and TDS were measured at the time of sampling using a digital multi-probe unit (model JE-3540). The samples collected were stored at 4 C° prior to analysis in the laboratory. In the laboratory, the chemical analyses were done by adopting standard procedures [7]. Total alkalinity was measured by titration with 1.6 N H$_2$SO$_4$ using phenolphthalein and bromocresol green-methyl red as indicators. Concentrations of HCO$_3^-$, Ca^{2+} and Cl$^-$ were also determined titrimetrically. The magnesium content was estimated by subtracting the calcium content from the total hardness. Sulfate and sodium

concentrations were determined by gravimetry (as a precipitate with $BaCl_2$) and flame photometry, respectively. During the analytical procedures, blanks and standards were run to check the reliability of the methods adopted. The charge balance was also applied to validate analyses with an acceptance limit of $\pm$ 10 % in meq/L. Results indicated that all samples satisfy charge balance within $\pm$ 5 %.

Hydrochemical data analysis

Hydrochemical data were represented graphically using stiff, scheoller and bar diagrams. These graphs were produced by using AquaChem ver 2011.1.40. Groundwater samples were also classified using the diagram proposed by Chadha (1999) [8]. Durov and cross plots (ionic ratios) diagrams were used to identify plausible hydrogeochemical processes controlling the groundwater composition. Visually communicating iso-concentration/contour maps were also constructed using ArcGIS-9.0 to delineate spatial variations of physico-chemical characteristics in groundwater samples. To get a better understanding of the hydrochemical processes and sources of solutes in the groundwater samples, two multivariate statistical techniques i.e. hierarchical cluster analysis (HCA) and principal component analysis (PCA) were applied. Hierarchical Cluster Analysis (HCA) comprises a series of multivariate methods, which is used to group the object based on the similar characteristics. Principal component analysis (PCA) is a multivariate technique that reduces a large number of variables to small ones, without sacrificing too much of the information [9, 10]. Prior to statistical analyses, all hydrochemical variables were z-scale standardized (the mean and variance were set to zero and one, respectively) to minimize the effects of different units and variance of variables and to render the data dimensionless. These analyses were performed SPSS (Version 21.0).

Results and Discussion

Hydrogeochemical characteristics of groundwater resources

Table 1 provides a statistical summary of the

Table 1. Major ions and physico-chemical characteristics of groundwater samples

Sample no	EC(μS/cm)	TDS	pH	TH	Na	Mg	Ca	SO$_4$	Cl	HCO$_3$
1	3300	2145	7.4	600	528	48	160	634	638	231
2	1540	1001	7.6	425	174	54	80	317	226	189
3	1336	868	7.7	350	149	42	70	302	148	183
4	2470	1606	7.5	600	231	72	120	509	460	170
5	6700	4355	7.4	3900	1439	826	200	3847	2100	238
6	7240	4706	7.1	1500	1092	145	360	903	1950	225
7	8780	5694	7.1	2000	1402	182	501	1302	2482	238
8	4500	2925	7.4	1000	675	121	200	489	1276	195
9	7480	4862	7.3	1100	1054	121	200	2185	1276	213
10	14950	9718	7.6	3750	2714	510	661	2853	4077	341
11	20000	13000	7.7	4000	1802	425	901	6912	2545	128
12	17130	11135	7.2	3500	3210	425	701	2512	5141	225
13	8870	5766	7.4	1500	2012	145	360	571	2836	189
14	2600	1690	7.6	550	395	60	120	610	439	189
15	4360	2847	7.8	800	781	97	160	7205	1143	207
16	6740	4331	7.2	1100	1264	121	240	922	1814	231
17	3560	2314	7.7	650	561	104	88	610	744	225
18	1630	1060	7.7	400	193	48	80	393	187	176
19	3218	2219	7.3	750	520	42	175	641	630	211
20	11610	7867	7.8	987	1425	816	198	3110	2115	203
21	14200	9749	7.1	870	2207	415	671	2107	4125	224
22	6691	4476	7.6	825	1107	135	375	875	1900	201
23	7110	4675	7.3	581	1102	152	510	875	1825	210
24	4500	3003	7.6	952	810	101	181	521	1210	171
25	6572	4600	7.4	1410	1115	107	215	1750	1215	198
Max	20000	13000	7.8	4000	3210	826	901	7205	5141	341
Min	1336	868	7.1	350	149	42	70	302	148	128
SD	5020	3301	0.23	3134	793	226	229	1881	1303	37
Arithmetic mean	7083	4664	7.4	1148	1118	212	314	1718	1700	208

All values are mg/l unless otherwise indicated

EC: Electrical Conductivity, TDS: Total Dissolved Solids, TH: Total Hardness (as CaCO$_3$), Min: Minimum, Max: Maximum, SD: Standard Deviation

physico-chemical parameters and major ions concentrations analyzed for this study.

Physico-chemical properties

In the study area, groundwater pH narrowly varied from 7.10 to 7.80 with an average value of 7.40, indicating neutral to slightly alkaline waters. The alkaline pH of groundwater samples marks that they have high ionic strength (TDS) and high buffering capacity. Supposedly, high cation exchange capacity of clay matrix (especially in central mudflat) as well as saturation with respect to calcite has increased the buffer capacity of these groundwaters and inhibits high pH variability.   As it is obvious from Figure 4a, the pH values gradually decrease along the groundwater flow path. A reasonable explanation for this trend is that groundwater in recharge area contains predominantly sulfate whereas in discharge area where ground-water

flow is very sluggish, chloride (more acidic species) becomes predominant.

The electrical conductivity (EC) of the groundwater is a rapid and good measure of dissolved solids (TDS) and is directly related to the concentration of ions present in the water. In the study area, EC varies considerably from 1336 to 20000 µS/cm (mean: 7083 µS/cm) and correspondingly TDS ranges from 868 to 13000 mg/l (mean 4664 mg/l). Based on these values, a vast majority (98 %) of all groundwater samples would be classified as brackish (TDS > 1000 mg/l) and 2% as freshwater (TDS < 1000 mg/l). As one can see in Figure 4b, EC shows an increasing trend along the groundwater flow direction. This is because of the long residence time of the water in the aquifer (as a result of low hydraulic gradient) and dissolution of reactive minerals in the alluviums through which water flows. In the study area, other hydrothermal mechanisms such as
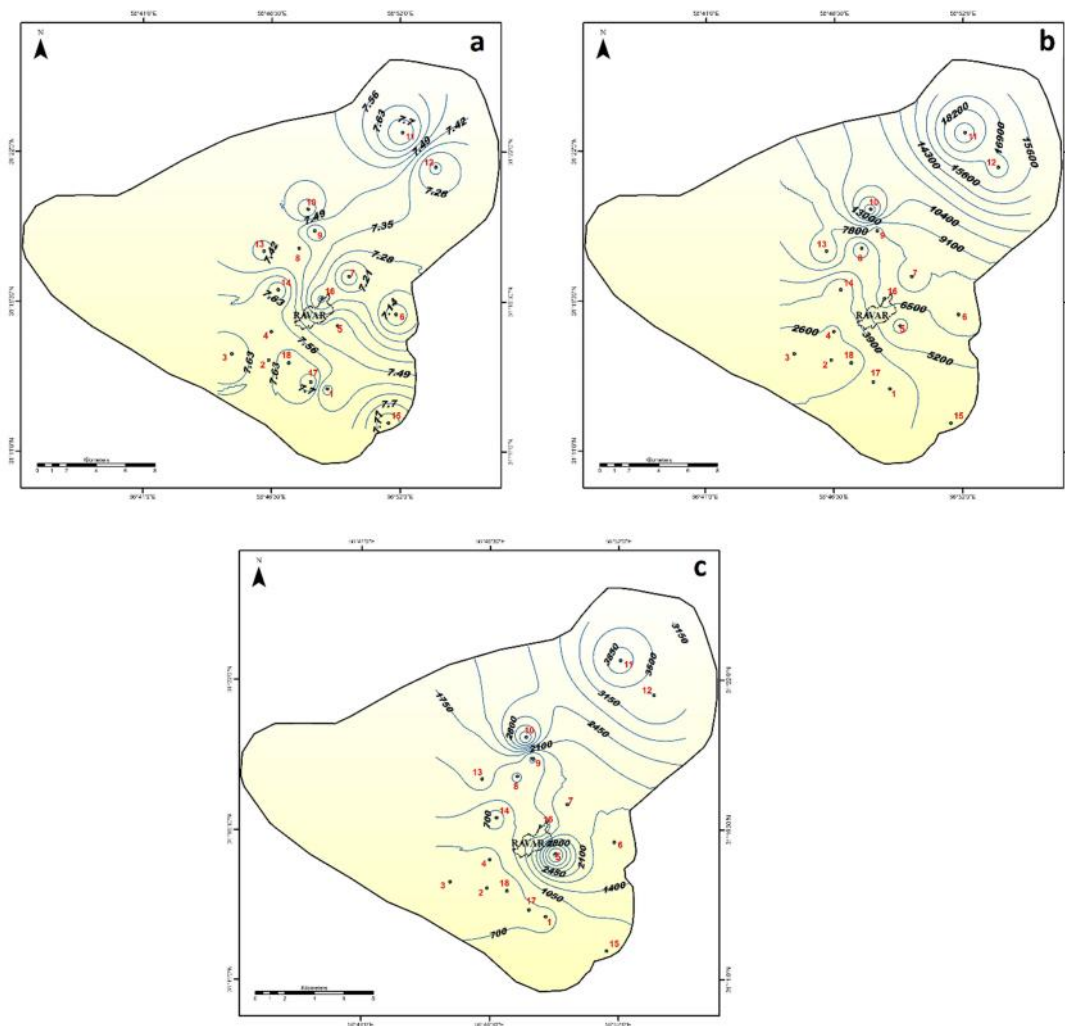

Figure 4. Distribution maps showing spatial variation in (a) pH, (b) EC and (c) TH of groundwater samples in the study area

Table 2. Classification of groundwater samples based on total hardness

Class	TH (as CaCO3)	Percentage of Samples
Soft	<75	---
Moderately hard	75–150	---
Hard	150–300	---
Very hard	>300	100%

evapotranspiration from the unsaturated zone especially near the flat playa, contribute to increased TDS levels in the groundwater resource.

The total hardness (TH) is another important parameter of water quality which is mainly due to presence of calcium and magnesium ions in water. The value of total hardness (as $CaCO_3$ equivalent) in the study area was found to be in the range of 350 mg/l to 4000 mg/l. The classification of groundwater (Table 2) based on total hardness (TH) shows that all the groundwater samples fall in the very hard water category. Therefore, most of the groundwater samples

with high (TDS >1000 mg/l) and TH (>300 mg/l) values can be classified as hard-brackish. As illustrated in Figure 4c, the TH values also increase in the direction of groundwater flow. Groundwater generally becomes hard and mineralized as it percolates through the unsaturated zone and moves through the groundwater system. It points again to effects of evaporation and dissolution of evaporitic (reactive) minerals by which the hardness and TDS of the groundwater are elevated.

Major ion chemistry

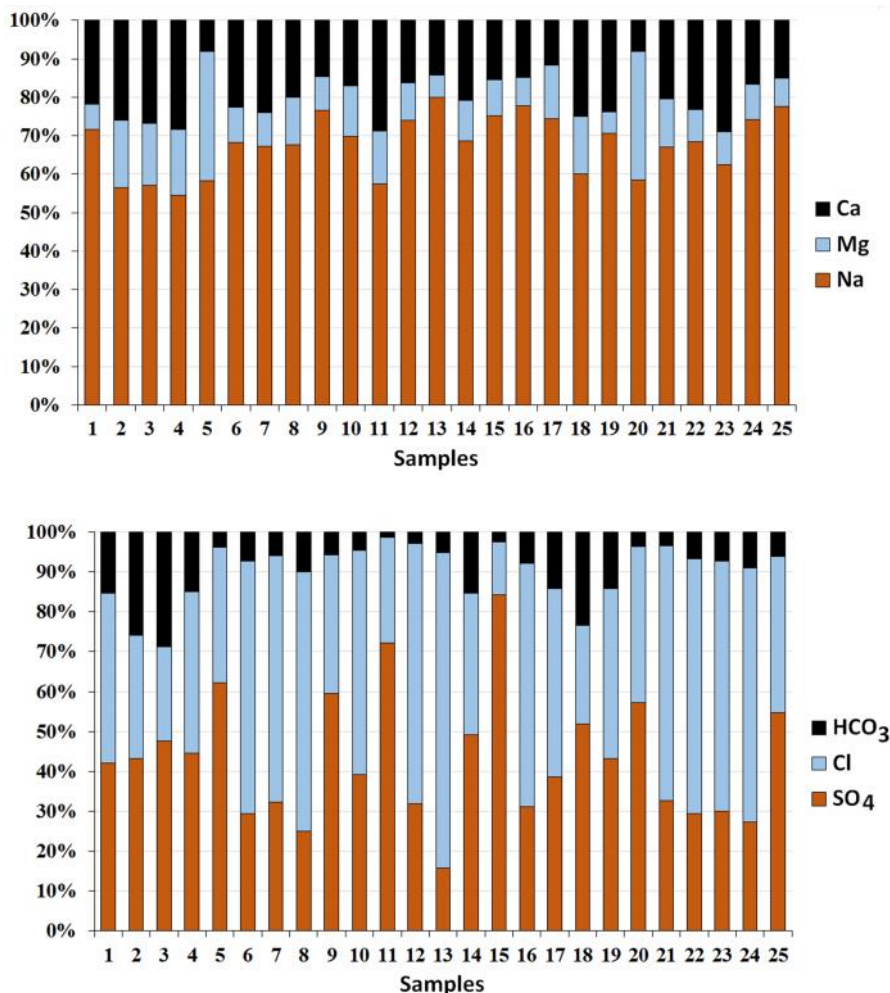Generally, major-ion chemistry of natural waters can

Figure 5. Percentage of major ions concentrations in groundwater samples

260

be explained by the reaction of the waters with rocks or sediments through which they flow. The chemical results obtained in the present study show that major ions occur within a wide range of concentrations in groundwater samples (Table 1). The concentrations of Ca^{2+}, Mg^{2+}, and Na^+ range from 70.14 to 908 mg/l, 42 to 826 mg/l, and 149 to 3816 mg/l, respectively. As it can be seen from Figure 5, sodium is the dominant cation followed by Ca^{2+} and Mg^{2+}. The concentrations of HCO_3^-, Cl^- and SO_4^{2-} vary from 2 to 341 mg/l, 148 to 5141 mg/l, and 302 to 6912 mg/l, with average 208, 1700 and 1718 mg/l, respectively. The order of abundance of the major anions is $Cl^- > SO_4^{2-} > HCO_3^-$. However, in some groundwater samples (no.5, no.11 and no.18), SO_4^{2-} is the predominant anion. Considering the watershed geology and groundwater flow path, it can be deduced that these major ions are mainly derived from the dissolution of evaporitic minerals or rocks salts (gypsum and halite) occurred in Ravar or Desu series or in other evaporite-bearing formations in the study area. Another contributing origin is the dissolution of evaporitic minerals which are being formed from evaporation process in the central mudflat. These will be discussed in detail in the following sections.

Plotting the results of groundwater chemical analysis on Schoeller's diagram (Figure 6) also revealed that the groundwater samples of the study area nearly had the same trend of major ion increase and decrease and are being more mineralized with respect to Na^+ and Cl^- ions as moving in the aquifer. HCO_3^- remains with little change, indicating some different processes limiting its increase. The distribution of SO_4^{2-}, Cl^-, Na^+, Ca^{2+} and Mg^{+2} in groundwater are similar to EC, which are high in the lower-lying northeastern parts and low in
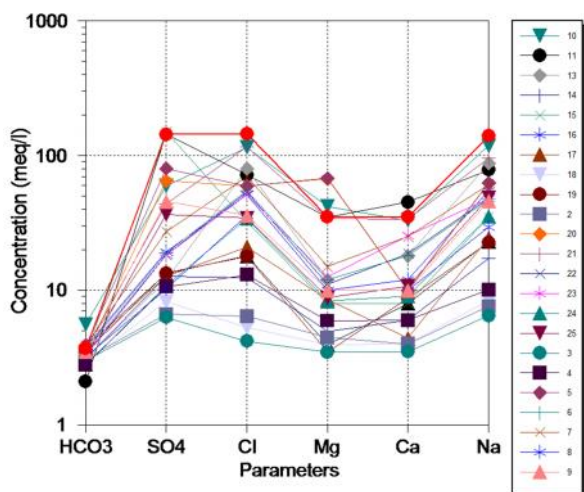
the southern parts of the plain. In other words, along the flow path of groundwater, the concentrations of all dissolved constituents (expect for HCO_3^-) tend to increase gradually. Such a trend is expected since groundwater as it moves along its flow path in the subsurface attains a high concentration of dissolved constituents [2]. However, the wide ranges of ion concentrations in this case indicate that several hydrochemical processes are involved in chemical evolution of groundwater in the study area.

Hydrochemical facies and groundwater classification

According to Stiff diagrams (Figure 7a), majority of the groundwater samples were classified as Na type of cation facies and Cl type of anion hydrochemical facies, respectively. However, few samples (accounting for <10.0 %) in the recharge area of the southern part of the study area are mainly of SO_4^{2-} water type as shown in Fig. 7a. No calcium or magnesium water types were identified in the study area. Based on the obtained results, it can be postulated here that composition and hydrochemical facies of groundwater change from the recharge regions to the discharge are and it generally evolves to Na-Cl type along the flow path. This is in agreement with the variation in TDS and EC along the
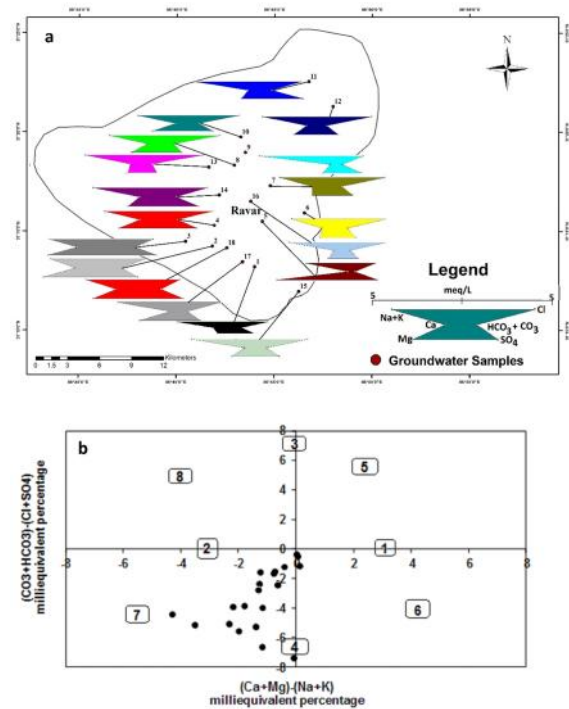

Figure 6. Logarithmic (Schoeller) diagram for groundwater samples

Figure 7. (a) Areal expression of Stiff diagrams for groundwater samples in the study area (for sake of clarity, 18 groundwater sampling sites are shown). (b) Classification of groundwater samples based on Chadha's diagram

direction of groundwater flow, suggesting the influences of evaporation, dissolution (water-rock interaction) and ion exchange processes which are able to increase the milliequivalent percentages of Na^+ and Cl^-, and decrease those of Ca^{2+} and HCO_3^- towards the discharge zone.

The groundwater is further evaluated to determine its facies by plotting the percentages of selected chemical constituents on Modified Piper diagram [8]. Chadha (1999) has proposed a new diagram for geochemical classification of natural waters and interpretation of water quality data. In this diagram, the difference in milliequivalent percentage between alkaline earths (calcium plus magnesium) and alkali metals (sodium plus potassium), expressed as percentage reacting values, is plotted on the X axis, and the difference in milliequivalent percentage between weak acidic anions (carbonate plus bicarbonate) and strong acidic anions (chloride plus sulphate) is plotted on the Y axis. The resulting figure is a square or rectangle, depending upon the size of the scales chosen for X and Y co-ordinates.

Our results clearly show that the majority of samples fall in seventh sub-field of the Chadha's diagram which reveals that alkali metals (Na^+) and strong acidic anions (Cl^-, SO_4^{2-}) exceed over alkaline earths (Ca^{2+}, Mg^{2+}) and weak acidic anions (HCO_3^-), respectively (Figure 7b). Such water generally creates salinity problems both in irrigation and drinking uses. The positions of data points in the proposed diagram represent Na –Cl–SO$_4$ type. The groundwater of this type with high TDS may be resulted from (1) the dissolution of soluble evaporitic minerals such as halite and gypsum (occurring in Desu or Ravar series or as products of evaporation process in the central mudflat area) and (2) Na/Ca exchange reactions occurring between the groundwater and fined grain-sediments particularly in mudflat zone. As the groundwater becomes more saline along its flow path, relatively insoluble salts (such as calcite) precipitate first and this explains HCO_3 depletion in the groundwater samples.

Hydrogeochemical mechanisms controlling groundwater composition

During groundwater movement along its path from recharge to discharge areas, a variety of hydrochemical reactions with solid phases takes place. Identifying and understanding these processes are essential for evaluating the causes of changes in groundwater quality. In this study, Gibbs' model, ion ratios, saturation indices for some eactive minerals and Durov diagram are all employed to identify the hydrochemical processes controlling the groundwater composition in the Ravar plain.

Gibbs model

Gibbs (1970) [11] has developed a diagram representing the ratios of $[(Na+K)/(Na +K +Ca)]$ as a function of TDS. This diagram gives a broad idea about the hydrochemical reactions influencing the groundwater chemistry. Based on Gibbs diagram, the hydro-chemical processes are classified into three types: evaporation–crystallization, rock–water interaction, and precipitation. As indicated in Figure 8a-b, most of the ground-water samples fall in the water–rock interaction field which suggests that groundwater chemistry in the study area are controlled, in a large part, by interactions between groundwater and minerals making up the aquifers. It is also obvious from Figure 7a-b that, there is a trend towards evaporation dominated field. The results obtained from the Gibbs diagram are further interpreted with following techniques to identify the exact chemical reactions that modify the chemical composition of groundwater in the study area.

Ionic Ratios

Compositional relations among dissolved species can reveal the origin of solutes and the processes that generated the observed water composition. The ionic ratios can act as a track-record of water–rock interaction
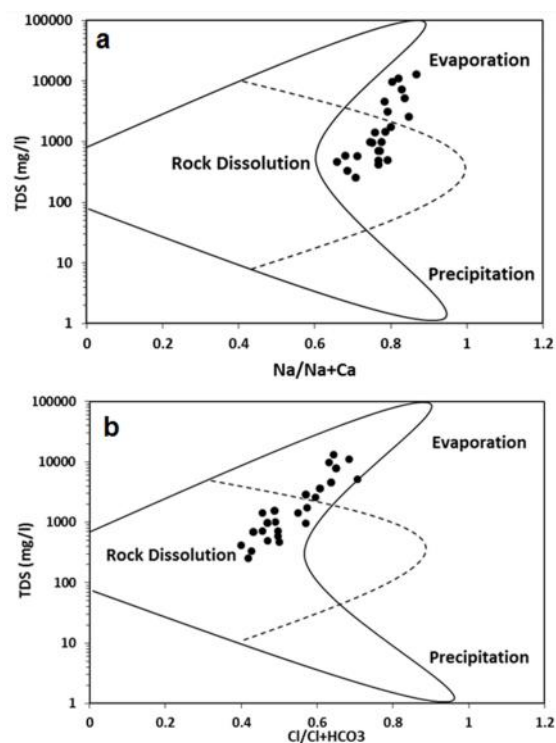

Figure 8. Gibbs plot of TDS values versus (a) Na/(Na +Ca) ratio and (b) Cl/(Cl +HCO$_3$) ratio for groundwater samples in the study area

Table 3. Major ionic ratios for groundwater samples in the study area

	Na/Cl	Ca/SO$_4$	CAI1	CAI2	Ca/HCO$_3$	Na/Ca	Cl/Br (molar)
1	1.27	0.60	-0.27	-0.29	2.10	2.87	715
2	1.18	0.61	-0.18	-0.12	1.29	1.89	491
3	1.54	0.55	-0.54	-0.24	1.16	1.85	101
4	0.87	0.56	0.22	0.22	2.14	1.67	179
5	1.05	0.12	-0.05	-0.035	2.56	6.258	676
6	0.86	0.95	-0.13	-0.33	4.86	2.63	2092
7	0.73	0.92	0.12	0.29	6.40	2.43	1055
8	0.93	0.98	-0.18	-0.49	3.12	2.93	429
9	1.27	0.21	-0.27	-0.20	2.85	4.58	2338
10	1.08	0.55	0.01	0.03	5.90	3.18	3828
11	1.22	0.31	-0.07	-0.05	21.43	2.04	4280
12	1.07	0.66	0.03	0.08	9.45	3.99	2557
13	0.98	1.51	-0.12	-0.66	5.80	3.88	2767
14	1.22	0.47	-0.38	-0.30	1.93	2.86	230
15	1.05	0.05	-0.05	-0.01	2.35	4.25	330
16	1.07	0.62	-0.07	-0.16	3.15	4.58	8887
17	1.16	0.34	-0.16	-0.20	1.18	5.54	1364
18	1.01	0.48	-0.01	-0.01	1.37	4.99	237
19	1.27	0.65	-0.27	-0.28	2.5	2.5	609
20	1.03	0.15	-0.03	-0.03	2.9	6.2	1076
21	0.82	0.76	0.17	0.42	9.1	2.8	1747
22	0.89	1.02	0.10	0.25	5.6	2.5	3965
23	0.93	1.39	0.06	0.16	7.4	1.8	1479
24	1.03	0.83	-0.03	-0.08	3.2	3.8	628
25	1.37	0.29	-0.37	-0.33	3.3	4.5	906
Mean	1.09	0.62	-0.09	0.03	4.54	3.40	3097
Min	0.73	0.05	-0.54	-0.16	1.16	1.67	101
Max	1.54	1.51	0.22	0.66	21.43	6.25	4280

during flow of groundwater in the subsurface [e.g., 12, 13]. For each particular situation, the selection of the more significant ratios to be studied should be made according to the possible sources of ions and the expected chemical processes along groundwater flow path. The ratios and parameters used to determine both the source rock and the chemical reactions are tabulated in Table 3 and discussed below**.**

Na/Cl ratio

Na/Cl ratio can be used to identify the mechanism of groundwater salinization in arid and semi-arid regions. If evapotranspiration and/or halite dissolution were responsible for the majority of sodium, then Na/Cl ratio should be approximately equal to 1, whereas ratios greater than 1 are typically interpreted as Na released sources other than halite dissolution or evaporation [14, 15]. For 83 % of the groundwater samples (Figure 9a), Na/Cl ratio is nearly equal to 1 and for 17 %, this ratio is much greater than 1. This indicates that for most groundwater samples, evaporation and subsequent dissolution of halite are the main processes modifying the groundwater chemical composition. This is consistent with predominated hydrochemical water type in the study area that is Na-Cl type. Evaporation from

the unsaturated zone leads to precipitation and deposition of evaporites that are eventually leached into the saturated zone. This greatly increases the concentration of ions in the groundwater leading to high salinity and TDS. Such a phenomenon is common in arid areas and presents potential source to salinization of groundwater systems. According to Jankowski and Acworth (1997) [16], if the evaporation process is dominant, assuming that the mineral species are precipitated, then Na/Cl ratio should be constant when EC increases. The EC versus Na/Cl scatter diagram of the groundwater samples (Figure 9b) shows that the trend line is virtually horizontal confirming that evaporation is one of the major controlling processes over groundwater quality at least for majority of the samples.

Ca/SO$_4$ ratio

Given the relative abundance of sulfate in groundwater samples, it can be assumed that gypsum is being dissolved in the groundwater system. This is confirmed by calculating the Ca/ SO$_4$ ratio for the groundwater samples. If the calcium and sulphate in groundwater are derived from dissolution of gypsum (or anhydrite), then the Ca/SO$_4$ ratio must be almost 1:1
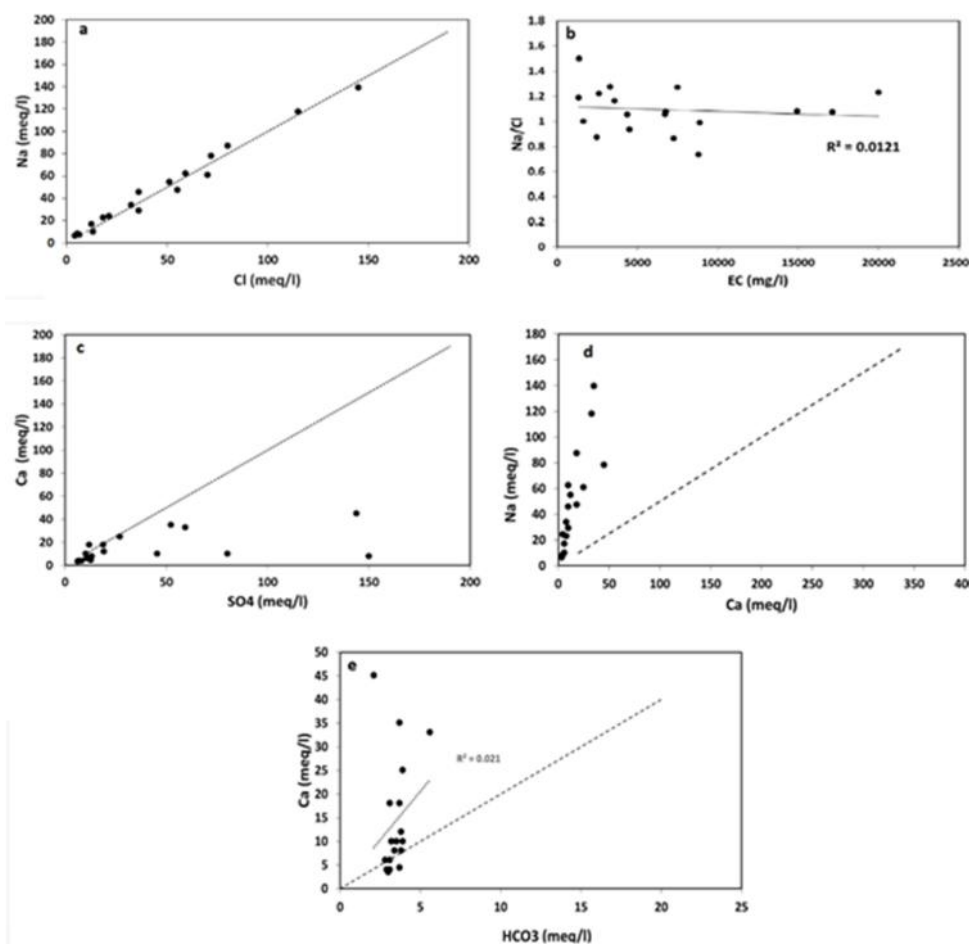
Figure 9. (a) Na versus Cl, (b) Na/Cl ratio versus EC, (c) Ca versus SO_4, (d) Na versus Ca and (e) Ca versus HCO_3

[17]. The majority of the water samples in the study area have Ca/SO_4 equivalent ratios close to unity, confirming that simple gypsum dissolution could exert a control on Ca^{+2} chemistry in the groundwater. In addition to abundance of gypsiferous rock units formed in the geological past (Desu and Ravar series and other evaporite-bearing sequences), mudflat (playa) sediments in the center and north of the Ravar plain are rich in evaporitic minerals (gypsum and halite). The formation of these soluble minerals is amplified in arid lands, such as the study area, due to the high evaporation rates and low rainfalls which encourage the precipitation of evaporitic minerals particularly in fine sediments of the playa deposits wherein capillary action is being taken place. As one can see from Figure 9c, several samples fall below the 1:1 trend line indicating that Ca^{+2} has been removed from the groundwater composition by other hydrochemical processes. Ca^{+2} derived from gypsum dissolution is probably involved in cation exchange for Na or removed through calcite precipitation.

To verify the hypothesis that ion exchange significantly affects groundwater compositions, chloroalkaline indices are computed [18]:

$$CAI\,1 = \frac{[Cl^- - (Na^+ + K^+)]}{Cl^-}$$

$$CAI\,2 = \frac{[Cl^- - (Na^+ + K^+)]}{SO_4^{-2} + HCO_3^-}$$

All values are expressed in meq/l. If the exchange takes place between Ca^{+2} in groundwater with Na^+ in the aquifer material, the indices will be negative, indicating normal ion exchange [18]. The results presented in Table 3 reveal that 8 % of the total samples have positive ratios and 92 % exhibit negative ratios. This suggests calcium from water is exchanged with sodium in the host rock (clay minerals in mudflat) favoring ion exchange reactions (chloroalkaline disequilibrium). The exchange of calcium for sodium on the clays can be represented by the following equation [14]: $Na_2 - Clay + Ca^{+2} \rightarrow 2Na^+ + Ca - Clay$

Ion-exchange process may be responsible for higher concentration of Na^+ in groundwater and this partly contributes to the groundwater salinization in the study area. It should be noted that in Na^+ vs. Ca^{2+} scatter diagram (Figure 9d), most of the groundwater samples fall above the equiline showing increased concentration of Na compared to Ca. This further strengthens the possibility of ion-exchange process involving in groundwater evolution in the study area.

Ca /HCO₃ ratio

The source of Ca in the groundwater can be further deduced from the Ca/HCO_3 ratio. Theoretically, the dissolution of calcite introduces Ca^{2+} and HCO_3^- ions into ground-water at a ratio of 1:1. As shown in Figure 9e, all groundwater samples in the present study are plotted above the 1:1 line, suggesting a relative abundance of Ca^{2+} over HCO_3^-. As this ratio increases with salinity, Ca^{2+} are added to solution at a greater rate than HCO_3. This reveals that calcium is derived from a source other than calcite (such as gypsum). This is also confirmed by the relatively low correlation between Ca^{2+} and HCO_3^- (r= 0.16, p<0.05). Therefore, it can be postulated that dissolution of carbonates is limited and it cannot be a major contributor to groundwater chemistry in the study area. Excess of Ca^{2+} is either removed through calcite precipitation or it is exchanged with Na adsorbed in aquifer matrix [2, 3], leaving behind excessive levels of SO_4^{2-} in groundwater. Occurrence of caliche (calcite cement) in the soil zone of the study area infer the long history of evaporation and precipitation of $CaCO_3$.

Solution–mineral equilibria

Mineral equilibrium calculations for groundwater are useful in predicting the presence of reactive minerals in the groundwater system and estimating mineral reactivity. These calculations provide an indicator called saturation index (S.I) for the minerals that may be reacting in the aquifer system.

Mathematically, S.I. is defined as the logarithm of the ratio of the ion activity product (IAP) to the mineral thermodynamic equilibrium constant (K_{sp}) adjusted to the temperature of the given sample and presented as $SI = \log(\dfrac{IAP}{K_{SP}})$. If SI<0, the groundwater is undersaturated (mineral dissolution condition), if SI>0 the groundwater is supersaturated (mineral precipitation condition) and if SI=0 the water is considered to be in equilibrium with respect to the particular mineral. In the present study, SI for common reactive minerals (calcite, dolomite, gypsum, and halite) was calculated by using PHREEQC interactive program [20]. The calculated values of SIs

Table 4. Saturation indices of groundwater samples with respect to reactive mineral phases

Stations	Gypsum	Calcite	Dolomite	Halite
1	-0.75	1.93	3.81	-5.13
2	-1.85	3.15	1.89	-6.02
3	-1.39	2.20	2.92	-6.26
4	-2.20	4.20	2.72	-5.61
5	-2.50	2.21	3.10	-4.22
6	0.11	3.52	1.28	-4.38
7	0.20	1.27	2.45	-4.19
8	-0.93	4.30	5.73	-4.74
9	0.43	5.10	6.04	-2.72
10	0.11	4.62	7.25	-3.67
11	-0.15	3.36	2.87	-3.59
12	-0.32	3.30	4.58	-4.09
13	-0.93	3.36	4.67	-5.41
14	-1.79	4.10	1.31	-4.48
15	-0.86	1.33	4.52	-4.73
16	-0.70	1.10	2.25	-4.34
17	-1.48	2.31	1.04	-5.04
18	-0.66	4.05	2.24	-4.71
19	-0.79	-0.17	-0.62	-5.14
20	-0.56	-0.41	0.14	-4.27
21	-0.19	3.18	0.50	-3.18
22	-0.55	4.03	-0.03	-4.39
23	-0.45	4.18	0.18	-4.14
24	-0.94	4.27	-0.44	-4.69
25	-0.50	5.20	-0.52	-4.57

for reactive mineral phases are presented in Table 4. Because of uncertainties in analytical and thermodynamic constants, water with a SI value between +0.5 and -0.5 is assumed to represent saturation conditions or is in equilibrium with respect to the mineral phase. The SI for dolomite varies between -0.62 and 7.25, that of calcite varies between -0.42 and 5.2 which indicates that nearly 80% of the groundwater samples are kinetically oversaturated with respect to calcite and dolomite. These results confirm that carbonate mineral phases are not being dissolved and their precipitation is likely. The saturation indices for evaporitic minerals fall near saturated to undersaturated state, ranging from 0.43 to -2.50 (for gypsum) and from -2.72 to -6.25 (for halite owing to its high solubility). This hints again that dissolution of evaporitic minerals exerts a significant control over groundwater chemistry in the study area.

Thermodynamically, dissolution of gypsum can induce calcite precipitation owing to common ion effect ($CaSO_4.2H_2O + 2HCO_3$ $CaCO_3 + SO_4 + H_2O + CO_2$). In fact once calcite reaches saturation, gypsum is still undersaturated and continues to dissolve, adding calcium and sulfate to the solution. Consequently, calcite becomes oversaturated and, as it precipitates, bicarbonate concentration decreases. The absence of Ca-HCO_3 groundwater type in the study area

supports this hypothesis. Furthermore, calcite precipitation may be also enhanced by evaporation process prevailing in the study area. Thus, the influx of Ca derived from the dissolution of gypsum causes increased Na concentrations as the cation-exchange reactions adjust to maintain equilibrium. With increasing TDS, the saturation indices of gypsum and halite increases, but those of calcite and dolomite remain relatively invariable, indicating that groundwater tends to dissolve gypsum and halite along the flow path (Figure 10), and the generated Ca leads to further precipitation of calcite.

Durov diagram

Durov's diagram was used to identify processes and

reaction paths such as mixing, cation exchange, and dissolution affecting groundwater composition. Hydrochemical reaction paths are indicated by the arrows on this diagram. Plotting of groundwater samples on the Durov diagram (Figure 11) shows that almost 75% of samples are quite close to the dissolution (mixing) line (arrow A) and 25% of the samples are aligned on arrow B (ion exchange reaction path Ca→Na apex) illustrating that both processes (dissolution and ion exchange) are actively involved in influencing the groundwater chemistry.

Statistical data analysis
The hierarchical cluster analysis (HCA)

The hierarchical cluster analysis (R-mode HCA) with
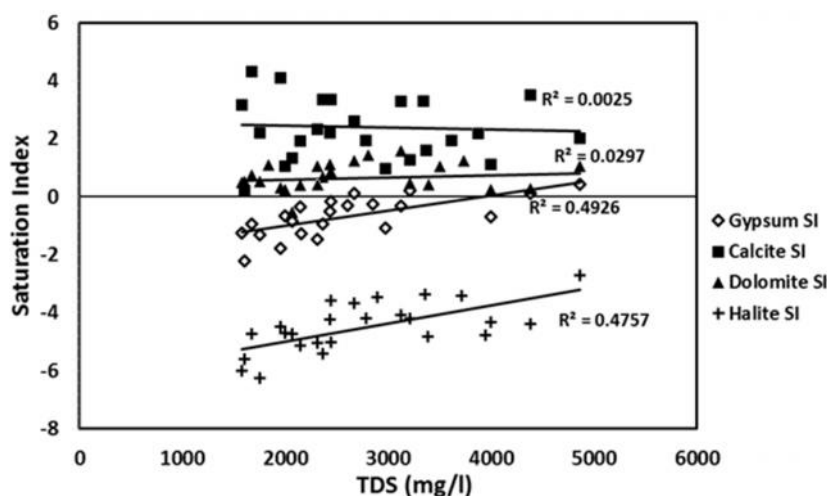

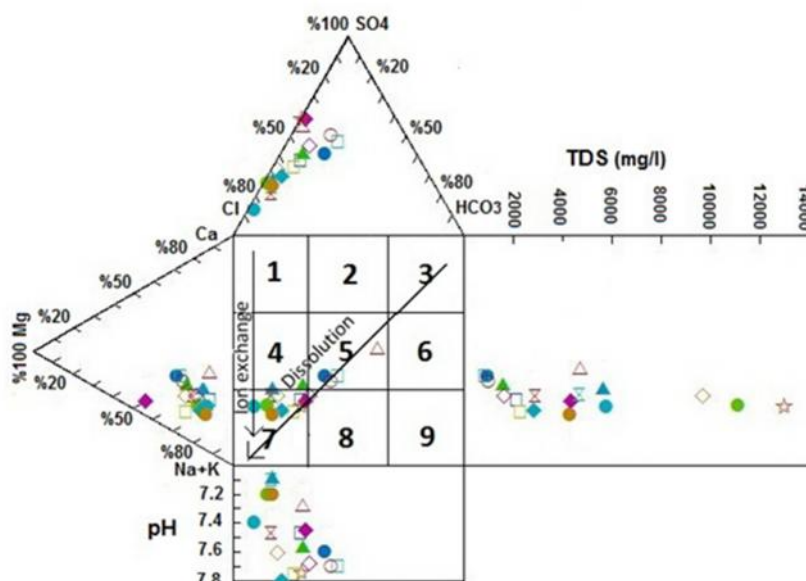**Figure 10.** TDS values versus saturation indices for reactive mineral phases

Figure 11. Durov Diagram depicting hydrogeochemical processes in groundwater of the study area
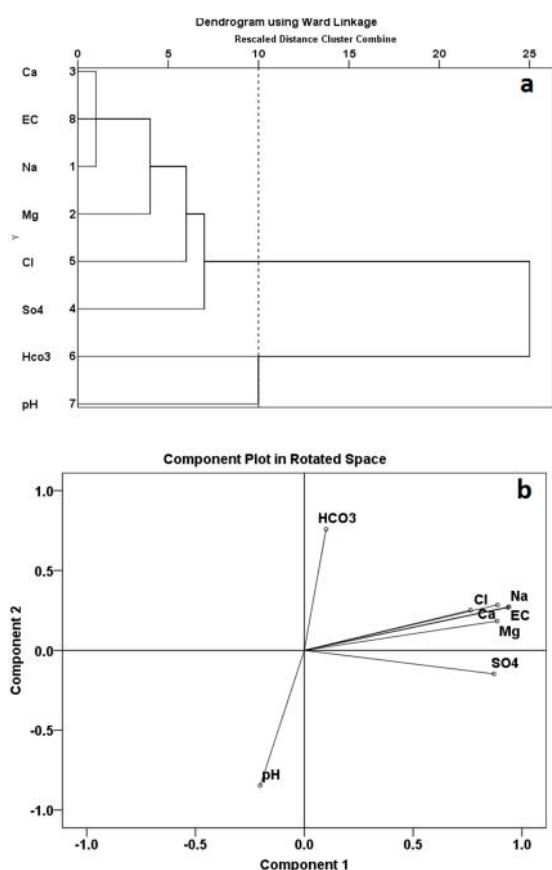
Figure 12. (a) Dendrogram of HCA classification. (b) Rotated space diagram showing the genetic affiliation of major hydrochemical parameters

Ward linkage was applied to identify clusters of 8 variables consisting of the main hydrochemical (pH, EC, HCO_3^-, Ca^{2+}, Mg^{2+}, Na^+, Cl^- and SO_4^{2-}) data. The result of such classification is visualized as a dendrogram in which the dissimilarity of the objects is represented by the height at which the branches are connected. A phenon line was drawn across the dendrogram at a linkage distance of about 10. The

position of the phenon line allows a division of the dendrogram into two clusters (Figure 12a). Cluster 1 includes Ca^{2+}, EC, Na^+, Mg^{2+}, Cl^- and SO_4^{2-} representing that these parameters are the main contributors to mineralization or salinization of groundwater and that they have a common source in groundwater (i.e. dissolution of evaporitic minerals and/or evaporation). Cluster 2 comprises only two variables pH and HCO_3^-. The presence of HCO_3^- and pH and the absence of Ca in the same cluster confirm that dissolution of calcite does not occur in the groundwater system and calcite precipitation is expected. As calcite precipitates, dissolved HCO_3^- concentration in groundwater decreases and pH increases.

Principal components analysis (PCA)

PCA was applied to obtain correlations among the hydrochemical constituents of groundwater samples [21]. The input data set consist of a 25 × 8 matrix, in which rows represent groundwater samples analyzed (25 objects), and columns display the specific analyzed parameters (8 variables; pH, EC, HCO_3^-, Ca^{2+}, Mg^{2+}, Na^+, Cl^-, SO_4^{2-}). Based on the eigenvalues (>1), two latent factors explaining 79.58% of the variance were extracted from the original data structure. The rotated factor loadings for each parameter are presented in Table 5 (values greater than 0.50 are in bold typeface). Figure 12b also shows the loading plot of PC 1 vs PC2. As it can be seen, the first component (PC1) was positively correlated with EC (0.94), Na^+ (0.93), Mg^{2+} (0.88), Ca^{2+} (0.88), SO_4^{2-} (0.87), Cl^- (0.76) and accounted for about 64.51 % of the total variance in the data set. The high loading factor of EC is likely due to the active participation of dissolved ions in the groundwater quality. The major variables constituting PC1 (i.e., Na^+, Cl^-, SO_4^{2-}, EC) are related to the hydrochemical variables originating from mineralization of groundwater. Therefore, the PC1 is interpreted as relating mainly to salinization (mineralization) of groundwater due to dissolution processes of evaporitic

Table 5. Loading factors and explained variance for the 2 principal components with Varimax normalized rotation

	PC1	PC2
Na	0.936	0.269
Mg	0.886	0.183
Ca	0.888	0.285
SO_4	0.871	-0.147
Cl	0.764	0.252
HCO_3	0.100	0.758
pH	-0.203	-0.846
EC	0.940	0.273
Eigenvalue	5.162	1.205
% of variance	64.519	15.062
Cumulative %	64.519	79.581

Absolute loading factors of more than 0.57 are marked in bold typeface

minerals (i.e. gypsiferous and halite layers in evaporite-bearing formations or from those being formed from the evaporation process in mudflat zone. Ion exchange process occurring in the mudflat area (where hydraulic gradient is low) can be a contributing process in changes of groundwater composition. The PC2 (with 15.06 % of the total variance) is characterized by high negative loadings of pH (-0.84) and HCO_3^- (0.75) indicating again that their levels in groundwater is controlled by calcite solubility limit. The PCA results are in perfect agreement with those obtained from HCA.

Conclusion

This study was conducted to evaluate the hydrochemical quality and to identify the most important hyrogeochemical processes controlling the groundwater quality in the Ravar plain (a typical arid area in southeastern Iran). The results indicated that groundwater in the study area was generally hard, alkaline and highly mineralized. The concentration of cations is in the order of $Na^+ > Ca^{2+} > Mg^{2+}$, while for the anions it is $Cl^- > SO_4^{2-} > HCO_3^-$. The concentrations of major dissolved constituents and hydrochemical parameters (EC, pH, TH) show a general tendency to increase along the groundwater flow direction. Na-Cl water type is found to be the prevalent hydrochemical facies in the study area. These finding suggests that evaporation and dissolution of evaporite minerals are the most important hydrochemical processes controlling the groundwater chemistry in the Ravar plain. These implications are confirmed by geochemical modeling using PHRREQC and calculation of some ionic ratios including Na/Cl, Ca/SO_4, Ca/HCO_3. Calcite and dolomite were found to be oversaturated in groundwater and to possess a precipitation tendency, while halite and gypsum were in unsaturated to saturated states and thus would dissolve during groundwater flow. Dissolution and precipitation of mineral phases determine the contribution to, and removal of, ionic species in solution. The multivariate statistical methods further support the hydrochemical interpretations.

Taking into account of all the obtained results of the study, it can be concluded that quality of groundwater resources in the Ravar plain is being naturally deteriorated. This situation can be worsened by human activities in future (particularly through over-abstraction, discharge of irrigation water flow and municipal wastewater). However, degradation of groundwater quality may be minimized if hydrochemical factors are understood and integrated in a management plan for these resources. Finally, the results of the present study also provide significant information on the groundwater quality situation and geochemical evolution of groundwater to local decision makers so that they can take sustainable groundwater management strategies for the highly vulnerable groundwater resources in this arid region.

References

1. Ward D. The Biology of Deserts. Oxford University Press, Oxford (2016).
2. Clark I. Groundwater Geochemistry and Isotopes. CRC press, New York (2015).
3. Appelo C.A.J. and Postma D. Geochemistry, Groundwater and Pollution. CRC press, Amsterdam (2005).
4. Modarres R. and Da Silva V.P.R. Rainfall trends in arid and semi-arid regions of Iran. *J. Arid .Environ.* **70**: 344–355 (2007).
5. Mahdavi A.E., Aghanabati A., Sohieli M., Mohajel M., Huckriede R. and Haj Mola Ali, A. Geological quadrangle map of Ravar (scale 1:250000). *Geological survey of Iran*, Tehran (1996).
6. Stocklin J. Lagoonal formations and salt domes in East Iran. *Bull. Iran. Pertrol. Instit.* **3**: 29–46 (1961).
7. APHA. Standard methods for the examination of water and wastewater. 21st ed. Washington: American Water Works Association, Water Environment Federation. p.541 (2005).
8. Chadha D.K. A proposed new diagram for geochemical classification of natural waters and interpretation of chemical data. *Hydrogeol. J.* **7**: 431–439 (1999).
9. Hassen I., Hamzaoui-Azaza F. and Bouhlila R. Application of multivariate statistical analysis and hydrochemical and isotopic investigations for evaluation of groundwater quality and its suitability for drinking and agriculture purposes: case of Oum Ali-Thelepte aquifer, central Tunisia. *Environ. Monit. Assess.***188**: 135-146 (2016).
10. Huang G., Chen Z. and Sun J. Water quality assessment and hydrochemical characteristics of shallow groundwater in eastern Chancheng district, Foshan, China. *Water. Environ. Res.* **2**: 354–362 (2013).
11. Gibbs R.J. Mechanisms controlling world's water chemistry. *Science* **170**: 1088–1090 (1970).
12. Wang X., Zhou X., Zhao J., Zheng Y., Song C., Long M. and Chen T. Hydrochemical evolution and reaction simulation of travertine deposition of the Lianchangping hot springs in Yunnan, China. *Quatern. Int.* **18**: 1–14 (2016).
13. Pasvanoglu, S. Hydrogeochemistry of thermal and mineralized waters in the Diyadin (Agri) area, Eastern Turkey. *Appl. Geochem.* **38**: 70–81(2014).
14. Hounslow A.W. Water quality data: analysis and interpretation. CRC Lewis Publishers, Florida (1995).
15. Pratheepa V., Ramesh S., Sukumaran, N. and Murugesan,

A.G. Identification of the sources for groundwater salinization in the coastal aquifers of Southern Tamil Nadu, India. *Environ.Earth.Sci.* **4**: 2819–2829 (2015).

16. Jankowski J. and Acworth R.I. Impact of debris-flow deposits on hydrogeochemical processes and the development of dryland salinity in the Yass River catchment, New South Wales, Australia. *Hydrogeol. J.* **5**: 71–88 (1997).

17. Ledesma-Ruiza R., Pastén-Zapataa E., Parraa, R., Harterb, T. and Mahlknecht J. Investigation of the geochemical evolution of groundwater under agricultural land: A case study in northeastern Mexico. *J. Hydrol.* **521**: 410–423 (2015).

18. Schoeller H. Les eaux souterraines Massio et Cie, Paris, France (1962).

19. Alcalá F.J. and Custodio E. Using the Cl/Br ratio as a tracer to identify the origin of salinity in aquifers in Spain and Portugal. *J. Hydro.* **359**: 189–207 (2008).

20. Parkhurst D.L. and Appelo C.A.J. User's guide to PHREEQC – A computer program for speciation, reaction-path, 1D-transport, and inverse geochemical calculations: Technical Report 99-4259. US Geological Survey, Denver, Colorado (1999).

21. Selvakumar S., Ramkumar K., Chandrasekar N., Magesh N.S. and Kaliraj K. Groundwater quality and its suitability for drinking and irrigational use in the Southern Tiruchirappalli district, Tamil Nadu, India. *Appl.Water. Sci.* doi: 10.1007/s13201-014-0256-9 (2014).

22. Kavab Engineering Consultants. A report on prohibition of water abstraction within Ravar plain. p.160 (2010).

23. Karimzadeh A., Aminizadeh Bazanjani M.R. Scrutiny of Feasibility of Implementation for Underground Dam in the Margin of Desert for Land Farming (Case Study, Kerman (Ravar) Underground Dam). IJABBR. **1**: 1129-1141 (2013).